POLITECNICO DI TORINO
Repository ISTITUZIONALE

Model-Based Design of a Control System for the Upgrade of Biogas with Zeolite Sorbent Reactors

(Article begins on next page)

19 April 2024

Model-Based Design of a Control System for the Upgrade of Biogas with Zeolite Sorbent Reactors*

Luigi Bisone[1], Sergio Bittanti[2], Silvia Canevese[3], Elahe Davarpanah[4], Antonio De Marco[1], Maurizio Notaro[3], and Valter Prandoni[3]

Abstract— To remove carbon dioxide from biogas so as to produce biomethane, a fixed-bed tubular reactor filled with a zeolite pelleted solid sorbent is considered. To generate biomethane continuously, three batch reactors are operated in coordinated cycles. The control system operates in a two-level structure: a high-level coordination algorithm determines the shift from a process stage to another for each single reactor and computes the setpoints for the low-level controllers of each reactor; the low-level controllers regulate the process variables, such as the inlet gas flow rate, the inlet or outlet gas pressure and the sorbent temperature, according to the setpoints.

In this paper, we first investigate the modelling of the batch process by means of mass, energy and momentum conservation equations. The concurrent adsorption of methane is also taken into account. The model parameters are identified by means of a two-stage procedure using experimental measurements from two plants, a laboratory-scale one located in Piacenza (Italy) and a pilot-scale one located in Camposampiero (Italy). With the identified model we design a control system for the coordination of three batch reactors.

I. INTRODUCTION

Biomethane as a fuel has properties comparable to those of natural gas, so it can be injected into the gas transport and distribution grid and it can be used in high-efficiency co-generation plants or in vehicle motors [1]. Biomethane can be obtained from biogas, which is produced by anaerobic digestion of organic substance, including rubbish and waste. Upgrading it to biomethane requires the removal of its 40-70 vol% carbon dioxide (CO_2) content. To this purpose, different technologies have been developed [2]–[5]. Here we focus on a purification process based on physical adsorption on solid pellets composed of synthetic 13X zeolite [6], [7].

[1]Luigi Bisone and Antonio De Marco are Process scientists, Milan, Italy lbis@inwind.it, antoniodemarco65@gmail.com

[2]Sergio Bittanti is with the Department of Electronics, Information Technology and Bioengineering, Politecnico di Milano, Milan, Italy, and CNR - The National Research Council of Italy sergio.bittanti@polimi.it

[3]Silvia Canevese, Maurizio Notaro and Valter Prandoni are with RSE (Ricerca sul Sistema Energetico) S.p.A., Milan, Italy {silviamaria.canevese, maurizio.notaro, valter.prandoni}@rse-web.it

[4]Elahe Davarpanah is a PhD student at the Department of Applied Science and Technology, Politecnico di Torino, Turin, Italy elahe.davarpanah@polito.it

The basic batch process takes place in a fixed-bed tubular reactor filled with pellets. It consists of three main stages: adsorption, regeneration and cooling, as will be detailed in Section II. Continuous production of biomethane is obtained by operating alternately and coordinately a set of reactors, in each of which the batch process is carried out in a cyclic way. Due to the duration of each stage, three reactors at least are needed (see Fig. 1): at each time instant, one reactor is in the adsorption stage, another one is in the regeneration (desorption) stage and another one is in the cooling stage (Fig. 2); a short idle stage may also be necessary for exact synchronous operation (see also [8]).

Herein we deal with the modelling, identification and control of a three-reactor upgrading system. After describing the operation of a single batch reactor (Section II), we discuss its chemical kinetics and identify the related unknown parameters (Section III). Such identification is based on data coming from experiments conducted in part with a laboratory-scale reactor located at RSE "Processes and catalytic materials" laboratory in Piacenza, Italy, and in part with a pilot-scale reactor unit which was tested in real operating conditions at the anaerobic digester of the Centre for the biological treatment of liquid and solid waste of the ETRA company, located in Camposampiero, near Padua, Italy. The overall model of a single reactor, including the main thermo-fluid-dynamic phenomena beside the chemical ones, is presented in Section IV. The control problem for three reactors working cyclically in a coordinate way can then be faced (Section V). Finally, Section VI illustrates the performance of the proposed control system. Conclusions are drawn in Section VII.

II. REACTOR DESCRIPTION AND OPERATION

The mentioned laboratory reactor and pilot-scale reactor unit are described in [5] and [8] respectively. The former (see Fig. 3) is a finned heat-exchanger tube, 0.97 m long with $0.9695 \cdot 10^{-3}$ m^2 cross section; the fins form eight peripheral parallel channels filled with zeolite sorbent pellets. The latter is 1 m long and it is composed of a set of inner extruded aluminium tubes, as shown in Fig. 1 of [8]. Each tube, with a 61.5 mm-wide square cross section, has eight parallel and independent channels for biogas. A cooling/heating fluid, water in this case, is adopted to control the sorbent temperature. In the tubes, the sorbent fills the space inside the peripheral channels, while water, supplied by an external refrigerating and heating circulator, flows through the central channel and it cools or heats the sorbent indirectly
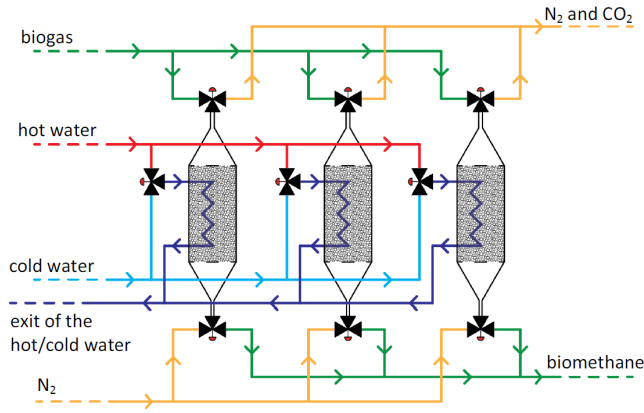
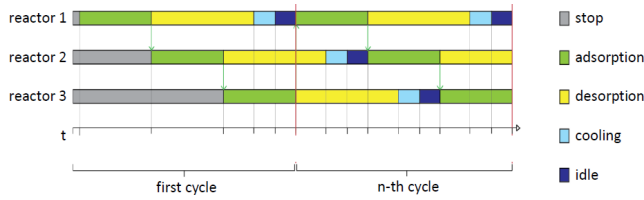Fig. 1. Process and instrumentation diagram of a three-reactor plant

Fig. 2. Timeline of the coordinated operation of three reactors; the desorption slot includes heating and depressurization
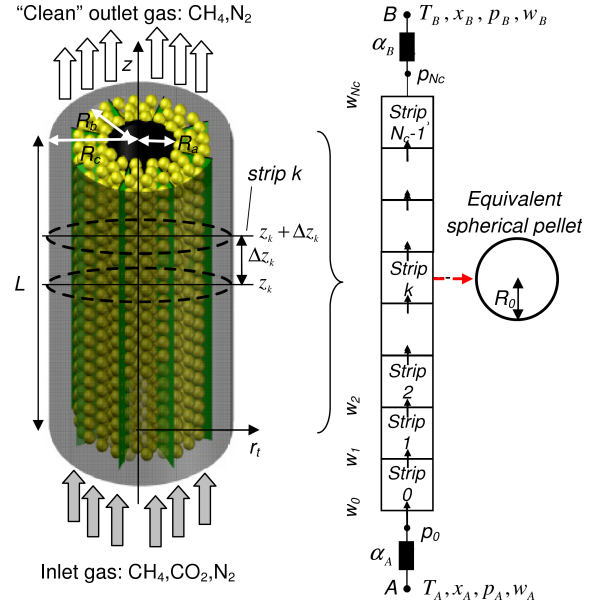

Fig. 3. Adsorption/desorption reactor: for modelling purposes it is divided into strips, in each of which the bulk gas and sorbent behaviour is described by suitable ordinary differential equations

by conduction, avoiding direct contact with it. An external jacket in series with respect to the tubes of the whole unit is fed with the thermal fluid exiting the tubes, and increases the surface for heat exchange with the sorbent. The lab reactor temperature is controlled in the same way, thanks to water circulating in its central channel (without pellets inside) and in an external jacket.

The sorbent is made up of highly porous approximately spherical zeolite pellets. The pellet radius is $R_0 = 0.001$ m, their mass density $\rho_p = 1358$ kg/m^3, their bulk mass density 626 kg/m^3, their overall bulk void fraction $\varepsilon_b = 0.5390$, their inner void fraction $\varepsilon_p = 0.4$. To treat biogas flow rates up to 1 Nm^3/h in the pilot plant, 6.835 kg of sorbent are employed. The laboratory reactor, instead, holds 0.589 kg of sorbent.

In the lab reactor, the sorbent temperature is measured by three type K thermocouples: one at the inlet section, one at the middle section and one at the outlet section. In the pilot-scale reactor, sorbent temperature is measured by means of forty-five thermocouples: fifteen at the inlet section, fifteen at the middle section and fifteen at the outlet section. For both reactors, gas composition is measured at the inlet and at the outlet by continuous analyzers. Both the temperature and gas composition measurements are recorded by a data logger with 1 Hz sample rate. The thermal fluid temperature and flow rate are controlled by means of the external refrigerating/heating circulator, which is equipped with a circulating pump. For reactor depressurization in the regeneration stage, a vacuum pump is adopted.

If CH_4 adsorption is neglected, i.e. if adsorption of CO_2 only is considered, the cyclic operation of each reactor unit can be thus described. The initial steady-state condition is characterized by no gas flow through the reactor and thermal fluid kept circulating and with temperature 25 °C. Then,

- at time $t_0 = 0$ s, the biogas valve at the inlet is opened, to start the adsorption stage. As the biogas flow crosses the reactor sections, adsorption takes place, on the sorbent inner porous surface; the circulating thermal fluid, with flow rate about 1320-1560 l/h and temperature controlled at 25 °C, partially takes away the released heat.
- When CO_2 starts to exit the reactor, e.g. when its molar fraction measured at the reactor outlet reaches a threshold (here 1%, which occurs roughly around time $t = 3600$ s for the pilot-scale unit), the adsorption stage is stopped, by closing the biogas valve. The regeneration stage is thus started. Here, N_2 (an inert gas) is injected into the reactor outlet (in a countercurrent fashion with respect to the previous biogas flow) and with a molar flow rate typically around 1/10 of the previous biogas molar flow rate. At the same time the circulating thermal liquid heating is started, so as to bring its temperature to 85-90 °C, and the reactor is depressurized. The depressurization is carried out by using the vacuum pump connected to the reactor inlet and discharging to the atmosphere. This leads to about 0.1 bar minimal pressure. One has to remark that desorption starts immediately, without waiting for the end of the fluid heating transient; the N_2 and CO_2 mixture exits from the reactor inlet and is sent to the atmosphere. In the pilot reactor, the regeneration stage is prolonged for 1 h, which means that there is no control of the complete regeneration status of the sorbent.
- Finally, the reactor is set to the cooling stage, by stopping the vacuum pump, closing the N_2 valve and

refrigerating the reactor by cooling the thermal liquid until the temperatures measured at the three mentioned sections reach the one set for adsorption, i.e. 25 °C, ± 2 °C. Now the reactor is put to the idle state, ready to begin a new adsorption stage.

As already hinted at, anyway, in the adsorption stage the considered zeolite does not capture CO_2 only, but also CH_4. We summarize, for instance, the results of some tests carried out at the ETRA site with 1 Nm^3/h inlet biogas flow rate, values of the inlet molar fractions typical for a good digester plant ($x_{CH_4} = 61\%$, $x_{CO_2} = 36\%$, $x_{N_2} = 2.7\%$, $x_{O_2} = 0.3\%$), reactor outlet pressure kept at the atmospheric value and temperature at 25 °C. Such tests show that, for the first 150-200 s, no CO_2 and no CH_4 exit the reactor, then (at $t = \tau_{d,CH_4} = 150$-200 s) CH_4 starts to exit, then (at $t = \tau_{d,CO_2} = 3000$-4000 s) CO_2 as well starts to exit. Sorbent regeneration carried out at 85 °C, with depressurization to 0.1 bar and 100 Nl/h stripping with N_2 shows that, anyway, it takes about 6 min only to desorb CH_4 (2 min to desorb most of it). In this way CH_4 can be recovered and employed, e.g. burnt. Even though the amount of adsorbed CH_4 is only some per cent of the inlet CH_4, it is useful to model the dynamics of the concurrent adsorption of CH_4 and CO_2. A deep analysis of the adsorption kinetics inside the zeolite sorbent is provided in the subsequent Section III.

III. CHEMICAL KINETIC MODEL: STRUCTURE AND IDENTIFICATION

As already pointed out, tests in the pilot plant indicate that, after the biogas valve opening to start the adsorption stage, CH_4 appears at the outlet with a breakthrough time (the mentioned τ_{d,CH_4}) of about 150 s. This is much more than the time needed by CH_4 to cross the reactor (about 6 s). Normally, the presence of CO_2 at the outlet always occurs with very high delays, since the sorbent affinity for CO_2 is much higher than that for CH_4. It should be noted that, in desorption tests, a simultaneous output of CO_2 and CH_4 is found, although with different percentages during the test. A possible interpretation of this phenomenon is that the adsorption sites for CH_4 are different from those for CO_2. Structurally, the kinetic equations for the two components can be assumed of the same Langmuir type [9] already mentioned in [10], that is, for $i = CO_2, CH_4$,

$$\phi_i \frac{\partial \theta_i}{\partial t} = K_{ads,i}(1 - \theta_i)C_i - K_{des,i}\theta_i\rho_{ref}, \qquad (1)$$

where $\rho_{ref} = p_{ref}/(R_g T_{ref})$. ρ_{ref} [$kmol/m^3$] is the reference molar density, $p_{ref} = 1.01 \cdot 10^5$ Pa the reference, atmospheric pressure, $T_{ref} = (20+273.15)$ K the reference temperature; R_g [$J/(kmol \cdot K)$] is the gas universal constant; ϕ_i [$kmol/m^2$] are the active sites available for component i, per unit surface; θ_i [$-$] is the fraction of sites occupied by component i, among those available for i; C_i [$kmol/m^3$] is component i molar concentration in the gaseous phase adjacent to the surface; $K_{ads,i}$ [m/s] and $K_{des,i}$ [m/s], respectively, are the adsorption and desorption coefficient for component i, between the surface and the gaseous phase.

The θ_i variables depend on space and time; they are assumed to become uniform in equilibrium steady-state conditions.

The unknown parameters in (1), namely $K_{ads,i}$, $K_{des,i}$ and ϕ_i, $i = CO_2, CH_4$, are now estimated from experimental data. The adopted approach and the related results will be described for the CO_2-related parameters first (Section III-A), then for the CH_4 ones (Section III-B).

A. CO$_2$-Related Parameters

As done in [10], a two-step approach is followed here: step 1 identifies the ratio of the CO_2 desorption and adsorption coefficients, i.e. $\eta_{CO_2} := K_{des,CO_2}/K_{ads,CO_2}$, step 2 identifies the two parameters K_{ads,CO_2} and K_{des,CO_2} individually, and also ϕ_{CO_2}.

The data for identification have been collected on the laboratory-scale reactor as follows. Nine adsorption tests have been carried out with CO_2 and N_2 inlet mixtures, with inlet volumetric flow rate Q_{test} = 287 Nl/h, inlet standard density (so that Q_{test} = 8.556·10^{-5} m^3/s) and at atmospheric pressure (throughout the reactor). Each test started with the sorbent carefully regenerated (i.e. $\theta_{CO_2} = 0$, throughout the reactor). Three different temperatures for the adsorption process have been considered, namely T_1, T_2, T_3 [K], corresponding to 20, 40 and 80 °C respectively; for each of them, a step of the inlet CO_2 molar fraction $x_{CO_2,in}$, from 0 to 5, 20 or 40%, has been executed. Steady-state values reached in all the tests have been employed in step 1 of the identification procedure, while the measured transient responses in three of those tests only have been employed in step 2.

In step 1, for each of the adsorption tests, we consider steady-state equilibrium conditions; therefore, in (1) $\partial\theta_{CO_2}/\partial t = 0$ and $\theta_{CO_2} := \theta_{CO_2,\infty}$ uniform along the reactor, as pressure and temperature are (almost) uniform. More precisely, the classical Langmuir equilibrium relation (see [11], p. 50) is obtained:

$$\theta_{CO_2,\infty} = \frac{\eta^*_{CO_2}x_{CO_2,in}}{\eta^*_{CO_2}x_{CO_2,in} + (T/T_{ref})(p_{ref}/p)}, \qquad (2)$$

where p [Pa] is the test pressure, here $p = p_{ref}$, and T [K] is the test temperature. $\eta^*_{CO_2} := \eta^{-1}_{CO_2} = K_{ads,CO_2}/K_{des,CO_2}$. Now, $\theta_{CO_2,\infty} = q_{ads,CO_2}/q_{max,CO_2}$, where q_{ads,CO_2} [g] is the equilibrium steady-state amount of CO_2 adsorbed in the test and q_{max,CO_2} [g] is the maximum amount of CO_2 which could be adsorbed, i.e. the amount adsorbed if all the sites were occupied. The value of q_{ads,CO_2} for each of the adsorption tests is reported in Table I. From such values and from (2) written for each test, $\eta^*_{CO_2}(T_j)$ and the related $q_{max,CO_2}(T_j)$, $j = 1, 2, 3$, are obtained, by minimizing the square error between the measured q_{ads,CO_2} values and the q_{ads,CO_2} values obtained from (2). The computed values are $\eta^*_{CO_2}(T_1) = 57.76$, $\eta^*_{CO_2}(T_2) = 28.66$, $\eta^*_{CO_2}(T_3) = 12.05$ and $q_{max,CO_2}(T_1) = 125.08$ g, $q_{max,CO_2}(T_2) = 113.34$ g, $q_{max,CO_2}(T_3) = 95.22$ g. We have thus three points $\eta^*_{CO_2}(T_j)$. The aim is to obtain, for $\eta^*_{CO_2}(T)$, a correlation decreasing monotonically with respect to temperature

T: therefore, we resort a cubic interpolation of $\eta^*_{CO_2}(T_j)$, $j = 1, 2, 3$. The identified q_{max,CO_2} values are adopted to estimate ϕ_{CO_2} in step 2.

As to step 2, we preliminarily recall that the available laboratory tests consist of a step variation of the inlet CO_2 molar fraction, at temperatures T_1, T_2 and T_3. The whole time responses of the CO_2 molar fraction leaving the reactor ($x_{CO_2,out}$) and of the sorbent temperature at the beginning and at the end of the reactor have been measured. The $x_{CO_2,out}$ responses allow to identify the two kinetic parameters K_{ads,CO_2} and K_{des,CO_2} individually and parameter ϕ_{CO_2}. Here the three tests with $x_{CO_2,in} = 40\%$ only are considered. The aim is to tune K_{ads,CO_2} and ϕ_{CO_2} so as to match, for each temperature, the $x_{CO_2,out}$ measured transient with the transient simulated by means of the overall reactor model (described in Section IV). More precisely, two quantities characterizing the transient of $x_{CO_2,out}$ have to be matched: $t_{1\%}$, i.e. the time, after the $x_{CO_2,in}$ step, after which $x_{CO_2,out}$ reaches 1%, and t_{fl}, i.e. the inflection point of the $x_{CO_2,out}$ transient. The aim is to find $K_{ads,CO_2}(T_j)$ and $\phi_{CO_2}(T_j)$ such that, for $j = 1, 2, 3$,

$$t_{1\%,mdl}(T_j) - t_{1\%,meas}(T_j) = 0$$
$$t_{fl,mdl}(T_j) - t_{fl,meas}(T_j) = 0, \quad (3)$$

where subscript $meas$ refers to the quantities associated to the measured transients and subscript mdl to the quantities associated to the corresponding simulated transients. In short, for each test, factor f_K related to diffusion into the sorbent micro-pores (see (10)) is computed first, and the values $\eta^*_{CO_2}(T_j)$ and $q_{max,CO_2}(T_j)$, $j = 1, 2, 3$ identified in step 1 are taken. An initial guess for $\phi_{CO_2}(T_j)$, $j = 1, 2, 3$, is derived from the relation $q_{max,CO_2}(T) = \phi_{CO_2}(T)A_{act}PM_{CO_2} \cdot 10^3$, where $PM_{CO_2} = 44$ kg/kmol is CO_2 molar weight and $A_{act} = G_m M_s$, where $G_m = 8 \cdot 10^5$ m^2 active surface/kg of sorbent and $M_s = 0.589$ kg is the sorbent mass in the lab reactor. A suitable initial guess for $K_{ads,CO_2}(T_j)$, $j = 1, 2, 3$ is also formulated. Then, the Newton-Raphson method is employed, starting from the guess values and computing the residues (3) and their Jacobian numerically. Few iterations suffice to obtain the three values $K_{ads,CO_2}(T_1) = 1.44 \cdot 10^{-10}$ m/s, $K_{ads,CO_2}(T_2) = 4.58 \cdot 10^{-10}$ m/s, $K_{ads,CO_2}(T_3) = 4.87 \cdot 10^{-10}$ m/s and the three values $\phi_{CO_2}(T_1) = 7.70 \cdot 10^{-9}$ kmol/m^2, $\phi_{CO_2}(T_2) = 5.94 \cdot 10^{-9}$ kmol/m^2, $\phi_{CO_2}(T_1) = 3.61 \cdot 10^{-9}$ kmol/m^2. Finally, $K_{ads,CO_2}(T)$ is chosen as a parabolic interpolation of the three values $K_{ads,CO_2}(T_j)$, $j = 1, 2, 3$; similarly, $\phi_{CO_2}(T)$ is chosen as a parabolic interpolation of the three values $\phi_{CO_2}(T_j)$, $j = 1, 2, 3$. $K_{des,CO_2}(T)$ is then obtained as $K_{des,CO_2}(T) = K_{ads,CO_2}(T)\eta_{CO_2}(T)$.

B. CH_4-Related Parameters

Reference is now made to one of the mentioned tests carried out at the pilot plant, since no tests with CH_4 in the inlet gas mixture are available for the lab reactor. The adsorption test was conducted with $Q_{test} = 1000$ Nl/h = 1 Nm^3/h, $x_{CH_4,in} = 58\%$, temperature 25 °C, pressure $p = p_{ref}$. From the measured transient of the outlet CH_4 molar fraction, one

TABLE I
LAB REACTOR: AMOUNT OF CO_2 ADSORBED IN THE NINE ADSORPTION TESTS

	$T_1 = 293K$	$T_2 = 313K$	$T_3 = 353K$
$x_{CO_2,in} = 40\%$	119.5 g	106.9 g	77.9 g
$x_{CO_2,in} = 20\%$	115.6 g	91.1 g	60.6 g
$x_{CO_2,in} = 5\%$	92.8 g	66.3 g	33.4 g

can obtain the adsorbed CH_4 quantity and the breakthrough time for CH_4, which is $\tau_{d,CH_4} \simeq 150$ s. The measured rising time τ_{rise} of the outlet CH_4 molar fraction to a value equal to the inlet CH_4 molar fraction appears to be very small. Let Q_{max,CH_4} [$kmol$] be the maximum CH_4 quantity which can be adsorbed. Starting from an initial guess for Q_{max,CH_4} and using a relation similar to (2), one can derive a first estimate for $\eta^*_{CH_4}$; of course, ϕ_{CH_4} is derived directly from Q_{max,CH_4}, via A_{act}. Then, a procedure similar to the one adopted in step 2 for CO_2-related parameters allows to obtain a refined estimate for Q_{max,CH_4} and an estimate for K_{ads,CH_4}. More precisely, the two parameters are identified so as to match the simulated outlet CH_4 molar fraction with the measured one in terms of τ_{d,CH_4} and τ_{rise}. In particular, the obtained K_{ads,CH_4} is $4.2675 \cdot 10^{-10}$ m/s. After that, $\eta^*_{CH_4}$ is derived from the new, refined Q_{max,CH_4}. Finally, from $\eta_{CH_4} := K_{des,CH_4}/K_{ads,CH_4}$ and the identified K_{ads,CH_4}, K_{des,CH_4} is derived.

C. Model Validation

The model with the identified parameters has been duly validated against the experimental data associated with the nine tests described above. To be precise, we have compared the outlet CO_2 molar fraction and the inlet and outlet sorbent temperature of the model with the measured transients. The obtained results are indeed very satisfactory; they cannot be reported herein, due to limitations in space.

IV. OVERALL REACTOR MODEL

As already mentioned, a batch reactor unit is composed of four parallel finned tubes, each of which is an elementary reactor composed of 8 smaller parallel channels with zeolite pellets inside. Similarly, the lab reactor is a finned tube, with 8 parallel channels to hold the zeolite pellets. We now describe the dynamic model adopted for such a reactor.

Distinct reference is made to two control volumes (cmp [5], [8], [10]): the bulk volume, consisting of the interstices among the pellets in the sorbent bed, and the sorbent volume itself with macro/meso-pores and micro-pores. The adopted zeolite sorbent, in fact, is obtained in the form of pellets by extrusion of crystalline zeolite powder. There are a lot of zeolite grains in a pellet; in each grain there are micro-pores where the CO_2 molecule can enter; spaces among grains, instead, are meso-pores, which are larger than micro-pores. CO_2 can be assumed to enter the meso-pores both by diffusion and via viscous flow. Transport from the meso-pores to the micro-pores is instead due to Knudsen's diffusion [9] only. Physical adsorption/desorption occurs inside

the porosity of the zeolite crystals. Both CO_2 and CH_4 are adsorbed. In the following, biogas is assumed as a mixture of CO_2, CH_4 and N_2.

The proposed model, reported in detail below, is based on one-dimensional Partial Differential Equations (PDEs), describing mass, momentum and energy conservation along the axial spatial coordinate z, plus algebraic constitutive relations. For numerical implementation, Ordinary Differential Equations (ODEs) have been worked out from such PDEs, by means of a standard finite-volume approach (cmp [8], [10]). More precisely, the reactor length L is divided into N_c strips (in the simulations here, $N_c = 861$) with identical width $\Delta z_k = \Delta z = L/N_c$, $\forall k = 0, \ldots, N_c - 1$ (Fig. 3), in each of which the bulk gas and sorbent behaviour is described by ODEs obtained by integrating the PDEs along z. We also recall that, in the ODEs for the bulk region, in each k-th strip, the "effect" of a single pellet is multiplied by the average number of pellets in the strip, i.e. $N_p \Delta z/L$, with N_p the total number of pellets in the reactor.

A. Hydrodynamic Model

The adopted equations for global, CO_2 and CH_4 mass conservation in the bulk volume read as

$$\frac{(\partial \rho A \varepsilon_b)}{\partial t} + \frac{\partial W_b}{\partial z} = -W'_{l,CO_2} - W'_{l,CH_4} \qquad (4)$$

$$\frac{\partial(\rho x_i A \varepsilon_b)}{\partial t} + \frac{\partial(W_b x_i)}{\partial z} = -W'_{l,i}, \quad i = CO_2, CH_4 \qquad (5)$$

where W_b [$kmol/s$] is biogas molar flow rate along z, ρ [$kmol/m^3$] is the bulk gas molar density, $W'_{l,i}$ [$kmol/s$] is component i molar flow rate, per unit length, entering the pellets pores (see Section IV-B), A [m^2] is the reactor cross section area and x_i [$-$] (or [%]) is component i molar fraction. Of course, $\forall t$ and $\forall z$, N_2 molar fraction is $x_{N_2} = 1 - x_{CO_2} - x_{CH_4}$.

Pressure appears to be almost uniform throughout the reactor (the overall pressure drop is about 5000 Pa), so pressure drops along the reactor can be neglected. As to the momentum and global mass accumulation terms in the bulk gas volume, namely the terms related to pressure and flow rate wave propagation, they can be assumed to have very small-time-scale dynamics; therefore, the quasi-steady state assumption is made here, which implies, e.g., that time derivatives in (4) and (5) are neglected. The same assumption is valid for the momentum and global mass conservation equations in the porous pellet volume.

Moreover, CO_2 and CH_4 concentrations in the meso-pores between the grains are assumed to be the same as their concentrations in the bulk gas flow through the reactor. This assumption is made since both the CO_2 and the CH_4 diffusive flow is substantially due to the concentration difference between meso-pores and micro-pores. Note that Knudsen diffusion is due to the molecules mean free path, so CO_2 diffusion is independent of CH_4 diffusion.

Remark: the dynamics of the reactor pressure depend mainly on the volumes of the manifolds at the reactor inlet and outlet; such manifolds are connected to control valves,

interception valves, etc. (see Fig. 1). Therefore, reactor pressure dynamics derive from the global mass conservation equation in the manifolds.

B. CO_2 and CH_4 Fluxes towards the Pellets: $W'_{l,i}$

The zeolite micro-pores are modelled here as cylindrical structures with average radius r_m [cm] and average length l_m [cm]. $r_m = 8 \cdot 10^{-8}$ cm (8 Å) for the adopted zeolite, l_m can be estimated from porosity measures. Since r_m is slightly higher than the average radius of the CO_2 molecule, CO_2 flow in the aforementioned cylinders is only diffusive, indeed it can be modelled as Knudsen's diffusive flow [9]: the CO_2 molar flow rate [$kmol/s$] towards a micro-pore is

$$J_{K,CO_2} = D_{K,CO_2}[\pi r_m^2/(l_m/2)](C_{b,CO_2} - C_{m,CO_2}) \qquad (6)$$

where D_{K,CO_2} (see [11], p. 136) is Knudsen's diffusion coefficient [cm^2/s] for CO_2, depending on the gas absolute temperature [K], on CO_2 molar weight [$kg/kmol$] and on r_m. C_{m,CO_2} is CO_2 concentration in each micro-pore inner volume and C_{b,CO_2} is the outer concentration which can be considered as the bulk one, since the micro-pores are assumed to be facing the bulk directly or to be facing macro-pores where CO_2 concentration can indeed be considered to be the same as the bulk concentration. A similar equation holds for J_{K,CH_4}.

We recall that $\phi_{CO_2}(\partial \theta_{CO_2}/\partial t)2\pi r_m l_m$ are the $kmol/s$ of CO_2 absorbed or desorbed by the micro-pore area. Thus, by neglecting mass accumulation in the micro-pore volume, in a steady-state approximation, one has

$$D_{K,CO_2}\frac{\pi r_m^2}{l_m/2}(C_{b,CO_2} - C_{m,CO_2}) = \phi_{CO_2}\frac{\partial \theta_{CO_2}}{\partial t}2\pi r_m l_m. \qquad (7)$$

One can then recall the kinetic equation

$$\phi_{CO_2}\frac{\partial \theta_{CO_2}}{\partial t} = K_{ads}(1 - \theta_{CO_2})C_{m,CO_2} - K_{des}\theta_{CO_2}\rho_{ref}, \qquad (8)$$

where $\phi_{CO_2}\theta_{CO_2}$ is the molar fraction of the occupied sites per m^2 on the micro-pores surface. Therefore, from (7) and (8), one obtains

$$\phi_{CO_2}\frac{\partial \theta_{CO_2}}{\partial t} = f_K K_{ads,CO_2}[(1 - \theta_{CO_2})C_{b,CO_2} + \\ -\eta_{CO_2}\theta_{CO_2}\rho_{ref}] \qquad (9)$$

$$f_K^{-1} = 1 + \frac{K_{ads}(1 - \theta_{CO_2})}{l_m^2/(D_{K,CO_2}r_m)}. \qquad (10)$$

Notice that (9) also means that, when $C_{b,CO_2} = 0$, θ_{CO_2} tends asymptotically to 0, as it can be expected from the process.

Finally, one has

$$W'_{l,i} = -\phi_i\frac{\partial \theta_i}{\partial t}A_{act}/L, \quad i = CO_2, CH_4, \qquad (11)$$

which shows that $\partial \theta_i/\partial t$ (> 0 during adsorption, < 0 during desorption), namely chemical kinetics, can be considered as the driving force both for adsorption and for desorption.

C. Thermal Model

The thermal model is composed of the energy conservation equations in the sorbent, bulk and cooling/heating system (i.e. the metal walls) control volumes [10]. They describe the dynamics of sorbent temperature $T_s(z,t)$ $[K]$, of bulk gas temperature $T_b(z,t)$ $[K]$ and of metal wall temperature $T_m(z,t)$ $[K]$. The former two equations read as

$$\frac{4}{3}\pi R_0^3 \rho_p c_s \frac{N_p}{L}\frac{\partial T_s}{\partial t} - \lambda_s \chi A \frac{\partial^2 T_s}{\partial z^2} = H_m \frac{A_{act}}{L}\phi_{CO_2}\frac{\partial \theta_{CO_2}}{\partial t} + $$
$$-4\pi R_0^2 \frac{N_p}{L}\gamma_{s,b}(T_s - T_b) - L_m \gamma_{s,m}(T_s - T_m) \tag{12}$$

$$\rho c_b A \frac{\partial T_b}{\partial t} + W_b c_b \frac{\partial T_b}{\partial z} = 4\pi R_0^2 \frac{N_p}{L}\gamma_{s,b}(T_s - T_b) + $$
$$-L_m \gamma_{b,m}(T_b - T_m), \tag{13}$$

respectively. In (12), on the left there are the energy accumulation term in the sorbent and the heat diffusion term in the sorbent along z, while the first term on the right is the power, per unit length along z, due to adsorption/desorption flux, the second term is the heat flux from the sorbent to the bulk, the third one is the heat flux from the sorbent to the heating/cooling system metal wall. In particular, c_s $[J/(kg \cdot K)]$ is the sorbent specific heat, λ_s $[W/(m \cdot K)]$ the sorbent thermal conductivity, χ $[-]$ a coefficient taking into account the contact area among pellets, i.e. taking into account how pellets in contact with each other transmit heat along z. H_m is CO_2 adsorption heat $[J/kmol]$, $\gamma_{s,b}$ $[W/(m^2 \cdot K)]$ the heat transfer coefficient between the sorbent and the bulk gas, $\gamma_{s,m}$ $[W/(m^2 \cdot K)]$ the heat transfer coefficient between the sorbent and the heating/cooling system metal wall, L_m the metal wall equivalent exchange perimeter [10]. In (13), on the left there are the energy accumulation term in the bulk gas and the convective energy transport term along z, while the first term on the right is the heat flux from the bulk to the sorbent and the second one is the heat flux from the bulk to the heating/cooling system metal wall. In particular, ρ $[kmol/m^3]$, we recall, is the bulk gas molar density, c_b $[J/(kmol \cdot K)]$ is the bulk gas molar specific heat, $\gamma_{b,m}$ $[W/(m^2 \cdot K)]$ the heat transfer coefficient between the bulk gas and the heating/cooling system metal wall. As to the cooling/heating system (i.e. the metal walls control volume), one of the classical models for heat exchangers has been adopted here [8], [10].

Finally, as to adsorption heat in standard conditions for CO_2, very precise measurements, carried out with *ad-hoc* test equipment, have yielded $H_m = 17 \cdot 10^6$ J/kmol. The adsorption heat for CH_4 has been neglected, instead, because, as already remarked, much less CH_4 than CO_2 is adsorbed.

V. REACTOR CONTROL

We recall that, in normal operating conditions, each reactor has to go through the different stages of the upgrading batch process in a cyclic way (see also [8]). Due to timing reasons (e.g., apart from the presence of the cooling stage after the regeneration one, the regeneration stage can last about twice

the adsorption stage), three reactors at least are needed to obtain an overall continuous process, producing a constant biomethane flow rate. As pointed out in Fig. 1 and Fig. 2, at each time instant there is a reactor in the adsorption stage where the CO_2 removal takes place. The other reactors operate in the other stages, to guarantee regeneration of the zeolite sorbent. A two-level hierarchical control structure can be an effective solution to handle a three-reactor plant. As in [8], for each reactor a high-level decision table is adopted to determine the transition from a stage to another and the setpoint values for the low-level control actions which characterize each stage.

In short, for each reactor, decision rules act, by switching them open/closed or on/off, on the inlet biogas interception valve, the outlet biomethane interception valve, the N_2 interception valve at the outlet, the interception valve to the atmosphere at the inlet, the interception valve toward the vacuum pump, the vacuum pump itself (assuming that there is one for each reactor), the water heating/cooling system. Such rules can be easily deduced from the description of the whole process given in Section II. For instance, the adsorption stage for a reactor is started by opening the interception valve for biogas at the reactor inlet and the one for biomethane at the reactor outlet; when the outlet CO_2 molar fraction reaches a threshold, say 1%, the biogas interception valve is closed and that reactor starts the regeneration stage, which also means opening the N_2 interception valve, starting the vacuum pump and starting water heating; after this stage, the reactor is put to the cooling stage by closing all its inlet and outlet valves, stopping the pump and starting water cooling; finally, the reactor is put to the idle stage, so as to mark its availability for the next adsorption stage.

As to the low-level controllers, during adsorption the biogas flow rate at the reactor inlet is controlled by a PI controller, via the rotation speed of a blower, while the biomethane pressure at the reactor outlet is controlled by the biomethane user (here, in particular, it is assumed to be kept constant, to 1 bar); water temperature is controlled by acting on the external circulator setpoint. Note that, since the adsorption stage follows the cooling stage of the previous cycle, water temperature is already 25 °C, because the circulator setpoint was switched to such a value at the beginning of the cooling stage. During desorption, pressure in the manifold at the reactor outlet is controlled via the rotation speed of the vacuum pump [8] (by varying the pressure setpoint; the control law is supplied by the pump manufacturer); the N_2 flow rate is controlled (kept constant) by a valve via an open-loop feed-forward action depending on the reactor pressure determined by the pump (N_2 pressure at the valve inlet is 1.2 bar).

VI. SIMULATION RESULTS

The cyclic behaviour of each reactor in a three-reactor system has been simulated, with a 0.1 s time step both for the reactor dynamic model and for the control actions, by using as input variables to the model the following basic data:
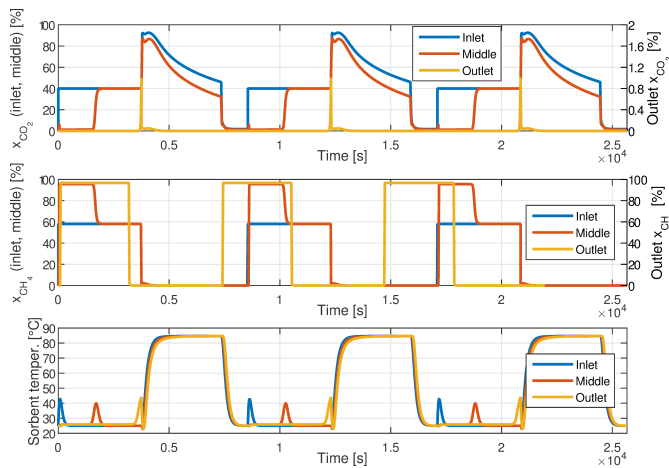
Fig. 4. Simulated variables for three consecutive full cycles, at the inlet, centre and outlet of one of the three reactors: from top to bottom, CO_2 and CH_4 molar fractions, sorbent temperature.

- water flow rate: 0.43 kg/s,
- setpoint for "hot" water temperature: 85 °C,
- setpoint for "cold" water temperature: 25 °C,
- setpoint for pressure during adsorption: $1.15 \cdot 10^5$ Pa,
- biogas volumetric flow rate: 100 Nl/h,
- CO_2 molar fraction in biogas: $x_{CO_2,in}$ = 40%,
- CH_4 molar fraction in biogas: $x_{CH_4,in}$= 58%,
- N_2 flow rate: 10 Nl/h,
- biogas temperature: 20 °C,
- setpoint for pressure during desorption: $0.1 \cdot 10^5$ Pa.

Such operating conditions are consistent with the ones in the mentioned tests carried out at the ETRA plant, and allow to obtain with the laboratory reactor model time dynamics similar to the ones typically found for the pilot-scale unit.

In Fig. 4, the simulated time evolution of the CO_2 and CH_4 molar fractions and of the sorbent temperature, all at the inlet, centre and outlet (namely in strip 0, 430 and 860) of one of the three reactors, are depicted during three adsorption-regeneration complete cycles. In each cycle, one can easily distinguish the adsorption stage, which lasts around 3600 s. Adsorption ends when CO_2 starts to exit the reactor, namely when its molar fraction at the outlet reaches the 1% threshold. The regeneration stage is then started. Thus, the sorbent temperature increases, up to 85 °C. The cooling stage is started after 3600 s from the beginning of regeneration and its duration is set to 1200 s. In the cooling period, the temperature controller cools water, and so the sorbent, down to 25 °C, to make the reactor ready for adsorption again. As to the sorbent temperature during adsorption, in particular, it shows some peaks which "follow" the gas flow along the reactor, from its inlet to its outlet; such peaks are consistent with adsorption of CO_2, which is seen both in terms of CO_2 molar fraction and in terms of the θ_{CO_2} variable (not reported, for brevity).

VII. CONCLUSIONS

The upgrade of biogas to biomethane is a main challenge of our times. In this paper we have studied a process based on a zeolite pelleted sorbent. The upgrade can take place by resorting to a control system for the coordination of a set of reactors operating alternately in order to ensure a continuous operation. To design this control system, we have constructed first a dynamic model of the cyclic CO_2 adsorption/desorption phenomenon. A problem worthy of supplementary investigation is tuning the control strategy to achieve a satisfactory compromise between process continuity, on the one hand, and the plant operating costs and the stress of the control variables, on the other hand.

REFERENCES

[1] I. U. Khan, M. H. D. Othman, H. Hashim, T. Matsuura, A. Ismail, M. Rezaei-DashtArzhandi, and I. W. Azelee, "Biogas as a renewable energy fuel - a review of biogas upgrading, utilisation and storage," *Energy Convers. Manag.*, vol. 150, pp. 277 – 294, 2017.

[2] M. Miltner, A. Makaruk, and M. Harasek, "Review of available biogas upgrading technologies and innovations towards advanced solutions," *J. Clean. Prod.*, vol. 161, pp. 1329 – 1337, 2017.

[3] K. Zhou, S. Chaemchuen, and F. Verpoort, "Alternative materials in technologies for biogas upgrading via CO_2 capture," *Renew. Sust. Energ. Rev.*, vol. 79, pp. 1414 – 1441, 2017.

[4] P. Castellazzi, M. Notaro, G. Busca, and E. Finocchio, "CO_2 capture by functionalized alumina sorbents: DiEthanolAmine on γ-alumina," *Micropor. Mesopor. Mat.*, vol. 226, pp. 444 – 453, 2016.

[5] L. Bisone, S. Bittanti, S. Canevese, A. De Marco, S. Garatti, M. Notaro, and V. Prandoni, "Modeling and parameter identification for CO_2 post-combustion capture by amines supported on solid sorbents," in *Proc. of the 19th IFAC World Congress*, Cape Town, South Africa, Aug. 24-29, 2014.

[6] J.-N. Kim, K.-T. Chue, K.-I. Kim, S.-H. Cho, and J.-D. Kim, "Non-isothermal adsorption of nitrogen-carbon dioxide mixture in a fixed bed of zeolite-X," *J. Chem. Eng. Jpn.*, vol. 27, no. 1, pp. 45–51, 1994.

[7] GRACE Davison. Material safety data sheet - according to 91/155 EEC, 2004. Last accessed: 3 November 2018. [Online]. Available: https://docs-emea.rs-online.com/webdocs/05a1/0900766b805a1998.pdf

[8] L. Bisone, S. Bittanti, S. Canevese, A. De Marco, and V. Prandoni, "Cyclic automation of a plant for the removal of CO_2 from biogas," in *Proc. of the 20th IFAC World Congress*, Toulouse, France, July 9-14, 2017.

[9] D. D. Do, *Adsorption Analysis: Equilibria and Kinetics*. Published by Imperial College Press and distributed by World Scientific Publishing Co., 1998.

[10] L. Bisone, S. Bittanti, S. Canevese, A. De Marco, S. Garatti, M. Notaro, and V. Prandoni, "A post-combustion carbon capture process by amines supported on solid pellets - with estimation of kinetic parameters," *Ind. Eng. Chem. Res.*, vol. 54, no. 10, pp. 2743–2762, 2015.

[11] D. M. Ruthven, *Principles of Adsorption and Adsorption Processes*. NY, USA: John Wiley & Sons, 1984.